

Teleportation-based realization of an optical quantum two-qubit entangling gate

Wei-Bo Gao,^{1,*} Alexander M. Goebel,^{2,*} Chao-Yang Lu,^{1,*} Han-Ning Dai,¹ Claudia Wagenknecht,² Qiang Zhang,¹ Bo Zhao,¹ Cheng-Zhi Peng,¹ Zeng-Bing Chen,¹ Yu-Ao Chen,^{1,†} and Jian-Wei Pan^{1,2}

¹*Hefei National Laboratory for Physical Sciences at Microscale and Department of Modern Physics, University of Science and Technology of China, Hefei, Anhui 230026, China*

²*Physikalisches Institut, Ruprecht-Karls-Universität Heidelberg, Philosophenweg 12, 69120 Heidelberg, Germany*

(Dated: October 31, 2018)

In recent years, there has been heightened interest in quantum teleportation, which allows for the transfer of unknown quantum states over arbitrary distances. Quantum teleportation not only serves as an essential ingredient in long-distance quantum communication, but also provides enabling technologies for practical quantum computation. Of particular interest is the scheme proposed by Gottesman and Chuang [Nature **402**, 390 (1999)], showing that quantum gates can be implemented by teleporting qubits with the help of some special entangled states. Therefore, the construction of a quantum computer can be simply based on some multi-particle entangled states, Bell state measurements and single-qubit operations. The feasibility of this scheme relaxes experimental constraints on realizing universal quantum computation. Using two different methods we demonstrate the smallest non-trivial module in such a scheme—a teleportation-based quantum entangling gate for two different photonic qubits. One uses a high-fidelity six-photon interferometer to realize controlled-NOT gates and the other uses four-photon hyper-entanglement to realize controlled-Phase gates. The results clearly demonstrate the working principles and the entangling capability of the gates. Our experiment represents an important step towards the realization of practical quantum computers and could lead to many further applications in linear optics quantum information processing.

In 2001, Knill, Laflamme and Milburn (KLM) showed that scalable and efficient quantum computation is possible by using linear optical elements, ancilla photons and post-selection [1]. The KLM scheme is based on three principles. First, non-deterministic quantum computation is possible with linear optics. Second, universal quantum gates with the probability approaching one can be implemented based on teleportation [5], a process in which a qubit in an unknown state can be transferred to another qubit [3, 4]. Third, the demanding resources can be reduced by quantum coding. The first principle has been demonstrated in many experiments. For example, various approaches for realizing photonic controlled-NOT (C-NOT) gates have been reported [1–3, 5–7, 11]. Recently, a three-qubit Toffoli gate has also been carried out in a photonic architecture [12]. Additionally, there have been many efforts aimed at reducing the resource requirements of the KLM protocol [13–16]. Nevertheless, the teleportation-based two-qubit entangling gate, which plays an important role in the second principle of the KLM scheme, still remains an experimental challenge.

Quantum teleportation is useful for quantum communication [17, 18] since it allows us to use entangled states as perfect quantum channels. The novel scheme proposed by Gottesman and Chuang (GC) in 1999 [5] opens the way for promising applications in realizing quantum computation (QC) [1, 5, 13, 14, 19]. In the GC scheme, qubits are teleported through special gates by simply

using multi-particle off-line entangled states, Bell state measurements (BSM) and single-qubit operations. It can be extended to implement universal measurement-based quantum computation. For example, in Refs. [13, 19], joint two-qubit measurements have been used to implement a teleportation-based model of quantum computation. It has also been shown that one-way quantum computation based on cluster states [20] is equivalent with the teleportation-based approaches [21, 22]. In addition, the GC scheme can be used to implement a nearly deterministic quantum gate. It teleports the qubits through a non-deterministic gate that has already been realized. Using more and more qubits, an entangling gate with a probability of success approaching one can be implemented [1].

To implement the fundamental building block of the GC scheme, teleportation-based C-NOT gate or controlled-Phase (C-Phase) gate, one has to use at least six qubits. All logic operations needed for quantum computation can be performed using single qubit operations in combination with a C-NOT gate or C-Phase gate [23]. In our experiment, we first realize a teleportation-based C-NOT gate with six photons. We measure the fidelities for the truth table of the gate and an entangled output state. Next, we implement a C-Phase gate by using a four-photon hyper-entangled state [24]. The fidelity of the gate is estimated. Moreover, we show that quantum parallelism is achieved in our C-phase gate, thus proving that the gate can not be reproduced by local operations and classical communications [25]. Our experiment represents a non-trivial proof-of-principle implementation of the teleportation protocol introduced by Gottesman and Chuang.

*These authors contribute equally to this work

†Current address: Fakultät für Physik, Ludwig-Maximilians-Universität, Schellingstrasse 4, 80798 München, Germany

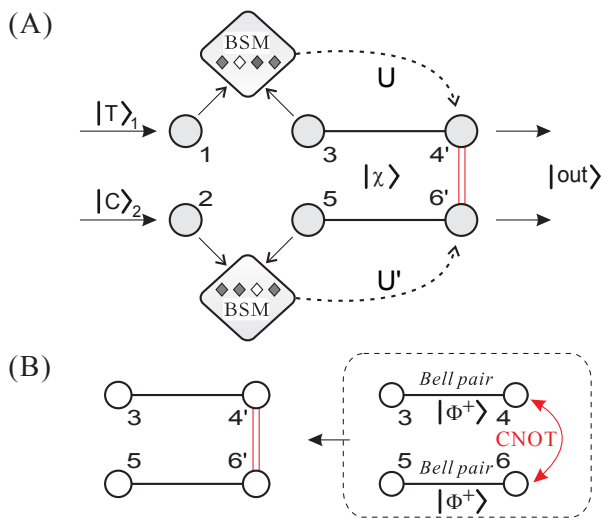


FIG. 1: Quantum circuit for teleporting two qubits through a C-NOT gate and a C-Phase Gate. (A) The input consisting of the target qubit $|T\rangle_1$ and control qubit $|C\rangle_2$ can be arbitrarily chosen. Bell State Measurements (BSMs) are performed between the input states and the left qubits of the special entangled state $|\chi\rangle$. Depending on the outcome of the BSMs, local unitary operations (U, U') are applied on the remaining qubits of $|\chi\rangle$, which then form the output $|out\rangle = U^{C-NOT}|T\rangle_1|C\rangle_2$ or $|out\rangle = U^{C-Phase}|T\rangle_1|C\rangle_2$. (B) The special entangled state $|\chi\rangle$ can be constructed by performing a C-NOT gate on two Bell pairs, with $|\Phi^+\rangle = \frac{1}{\sqrt{2}}(|H\rangle|H\rangle + |V\rangle|V\rangle)$. See Appendix for details.

I. THEORETICAL SCHEMES

A key element in the scheme of Gottesman and Chuang is to implement the C-NOT gate, which acts on a control and a target qubit. Here the logic table of the C-NOT operation (U^{C-NOT}) is given by $|H\rangle_1|H\rangle_2 \rightarrow |H\rangle_1|H\rangle_2$, $|H\rangle_1|V\rangle_2 \rightarrow |V\rangle_1|V\rangle_2$, $|V\rangle_1|H\rangle_2 \rightarrow |V\rangle_1|H\rangle_2$ and $|V\rangle_1|V\rangle_2 \rightarrow |H\rangle_1|V\rangle_2$, where we have encoded qubits on the polarization degree of freedom of photons. A schematic diagram of the procedure is shown in Fig. 1A. First, we prepare beforehand an entangled four-qubit state $|\chi\rangle$. Next, by using quantum teleportation, we transfer the data of the two input qubits $|T\rangle_1$ (target) and $|C\rangle_2$ (control) onto $|\chi\rangle$. Specifically, this is done by projecting the target (control) qubit and one of the outer qubits of $|\chi\rangle$ onto a joint two-particle ‘‘Bell state’’. To finish the procedure, we apply single qubit (Pauli) operations to the output qubits depending on the outcomes of the BSMs. Now the output is in the desired state given by

$$|out\rangle = U^{C-NOT}|T\rangle_1|C\rangle_2. \quad (1)$$

This can be better understood by a closer look at the special entangled state $|\chi\rangle$. It is a four-particle cluster

state [26] of the form

$$|\chi\rangle = \frac{1}{2}[(|H\rangle_3|H\rangle_{4'} + |V\rangle_3|V\rangle_{4'})|H\rangle_5|H\rangle_{6'} + (|H\rangle_3|V\rangle_{4'} + |V\rangle_3|H\rangle_{4'})|V\rangle_5|V\rangle_{6'}], \quad (2)$$

which can be created simply by performing a C-NOT operation on two EPR pairs $|\Phi^+\rangle = \frac{1}{\sqrt{2}}(|H\rangle|H\rangle + |V\rangle|V\rangle)$ (see Fig. 1B). Note that application of this C-NOT operation onto the two EPR pairs prior to teleportation is the reason that the input states have undergone a CNOT gate after teleportation. This is the essential difference between our scheme and standard teleportation. A detailed discussion of the scheme is shown in the Appendix.

When the off-line entangled resource is prepared in a different state, we can teleport the input qubits through a different entangling gate. For example, we prepare the off-line state as

$$|\chi'\rangle = \frac{1}{2}[(|H\rangle_3|H\rangle_{4'} + |V\rangle_3|V\rangle_{4'})|H\rangle_5|H\rangle_{6'} + (|H\rangle_3|H\rangle_{4'} - |V\rangle_3|V\rangle_{4'})|V\rangle_5|V\rangle_{6'}], \quad (3)$$

which results from performing a C-Phase gate between two EPR pairs $|\Phi^+\rangle$. Here the logic table of the C-Phase operation is given by $|H\rangle|H\rangle \rightarrow |H\rangle|H\rangle$, $|H\rangle|V\rangle \rightarrow |H\rangle|V\rangle$, $|V\rangle|H\rangle \rightarrow |V\rangle|H\rangle$ and $|V\rangle|V\rangle \rightarrow -|V\rangle|V\rangle$. After the creation of the entangled state $|\chi'\rangle$, we implement BSMs on qubit $|T\rangle_1$ with qubit 3, and qubit $|C\rangle_2$ with qubit 5. Based on the results of the BSMs, 16 possible Pauli corrections (See Appendix) are applied on qubits $4'$ and $6'$. This allows us to teleport the two qubits through a C-Phase gate. Note that the two types of entangling gates are equivalent up to single qubit unitary transformations. For example, by applying two Hadamard gates on one of the input qubits and the corresponding output qubit after teleportation, the C-Phase gate can be converted to a C-NOT gate.

II. THE EXPERIMENTAL DEMONSTRATION WITH SIX PHOTONS

A. The creation of the four-photon state $|\chi\rangle$

The C-NOT gate is implemented by using six photons. A schematic diagram of the experimental setup is shown in Fig. 2. All three photon pairs are originally prepared in the Bell-state $|\Phi^+\rangle = \frac{1}{\sqrt{2}}(|H\rangle|H\rangle + |V\rangle|V\rangle)$. We observe on average 7×10^4 photon pairs per second from each (EPR) source with a visibility of 87.5%. With this high-intensity entangled photon source we obtain in total 3.5 six-photon events per minute. This is less than half the count rate of our previous six-photon experiments [28, 29]. Since the new scheme is more complex and involves more interferences, the fidelity requirements are more stringent. Thus, we reduce the pump power from 1.0 W to 0.8 W in order to reduce noise contributions

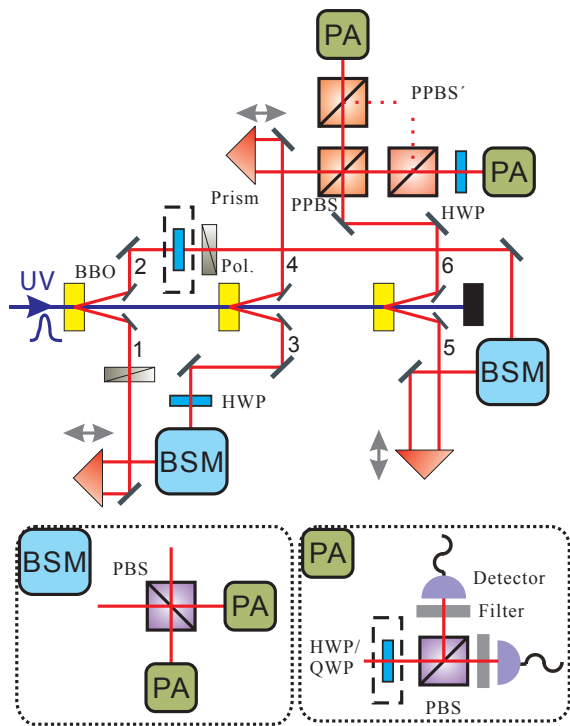


FIG. 2: A schematic diagram of the experimental setup. We frequency double a mode-locked Ti:sapphire laser system to create a high-intensity pulsed ultraviolet (UV) laser beam at a central wavelength of 390 nm, a pulse duration of 180 fs, and a repetition rate of 76 MHz. The UV beam successively passes through three β -barium borate (BBO) crystals to generate three polarization entangled photon pairs via type-II spontaneous parametric down-conversion [27]. At the first BBO the UV generates a photon pair in modes 1 and 2 (i.e. the input consisting of the target and control qubit). After the crystal, the UV is refocused onto the second BBO to produce another entangled photon pair in modes 3 and 4 and correspondingly for modes 5 and 6. Photons 4 and 6 are then overlapped at a PPBS and together with photons 3 and 5 constitute the cluster state. Two PPBS' are used for state normalization. The prisms are mounted on step motors and are used to compensate the time delay for the interference at the PPBS and the BSMs. A BSM is performed by overlapping two incoming photons on a PBS and two subsequent polarization analyses (PA). A PA projects the photon onto an unambiguous polarization depending on the basis determined by a half or quarter wave plate (HWP or QWP). The photons are detected by silicon avalanche single-photon detectors. Coincidences are recorded with a coincidence unit clocked by the infrared laser pulses. Polarizers (Pol.) are polarizers used to prepare the input state and narrow band filters (Filter) with $\Delta_{FWHM} = 3.2$ nm are used to obtain a better spectral interference.

from the emission of two pairs of down-converted photons by a single source (double-pair-emission).

Using wave plates and polarizers, we prepare photon pair 1&2 in the desired two-qubit input state $|\Psi\rangle_{12}$. Photon pairs 3&4 and 5&6, which are both in the state $|\Phi^+\rangle$, are used as resources to construct the special entangled

state $|\chi\rangle$. In the experiment, we use a two photon C-NOT gate to produce the desired cluster state [1–3, 30]. As shown in Fig. 2, photons 4 and 6 are interfered on partially polarizing beam splitters (PPBS), i.e. the transmission for the horizontal (vertical) polarization is $T_H = 1$ ($T_V = 1/3$). In order to balance the transmission for all input polarizations, PPBS' with reversed transmission conditions ($T_H = 1/3$, $T_V = 1$) are placed in each output of the overlapping PPBS. Altogether, the probability of having one photon in each desired output, and thus of having successfully created the cluster state, is $1/9$. Half wave plates (HWPs) in arms 3 and 4 are used to transform the cluster state to the desired state by local unitary operations.

To achieve good spatial and temporal overlap, the photons are spectrally filtered with very steep edge narrow-band filters ($\Delta\lambda_{FWHM} = 3.2$ nm) and detected by fibre-coupled single-photon detectors. At the same time, by shortening the distance between the BBO and the fiber coupler, and carefully refocusing the UV pulse with appropriate lenses, we are able to obtain an overall efficiency of about 15% (including the coupling and detection efficiency). The experimental count rate for the four-qubit cluster state $|\chi\rangle$ is $7/s$, which is two orders of magnitude larger than in a recent experiment [4]. Using the same method as ref. [4], we measure the state fidelity to be 0.694 ± 0.003 , which is slightly lower than that in [4]. The imperfect preparation of the desired cluster state is mainly limited by high-order emissions of entangled photons, the imperfect interference on PPBS and as well as the quality of PPBS, whose transmission ratio for different polarization is measured to be about $T_H = 0.95$ and $T_V = 0.3$ for one input and $T_H = 0.96$ and $T_V = 0.35$ for the other input.

B. Teleporting two qubits through a C-NOT gate

Teleporting the input data of $|\psi\rangle_{12}$ to $|\chi\rangle$ requires joint BSMs on photons 1&3 and photons 2&5. To demonstrate the working principle of the teleportation-based C-NOT gate, it is sufficient to identify one of the four Bell states in both BSMs [28, 32]. However, in the experiment we choose to analyse the two Bell states $|\Phi^+\rangle$ and $|\Phi^-\rangle$ to increase the efficiency - the fraction of success - by a factor of 4. This is achieved by interfering photons 1&3 and photons 2&5 on a polarizing beam splitter (PBS) and performing a polarization analysis (PA) on the two outputs [33]. With the help of a HWP, a PBS and fibre-coupled single photon detectors, we are able to project the input photons of the BSM onto $|\Phi^+\rangle$ upon the detection of a $|+\rangle|+\rangle$ or $|-\rangle|-\rangle$ coincidence, and onto $|\Phi^-\rangle$ upon the detection of a $|+\rangle|-\rangle$ or $|-\rangle|+\rangle$ coincidence (where $|\pm\rangle = (|H\rangle \pm |V\rangle)/\sqrt{2}$). The increase in success efficiency in comparison with Ref. [28, 32] allows us to reduce the pump power in order to reduce noise contributions while preserving the overall count rate. Note that even with a $1/4$ success probability of the BSM,

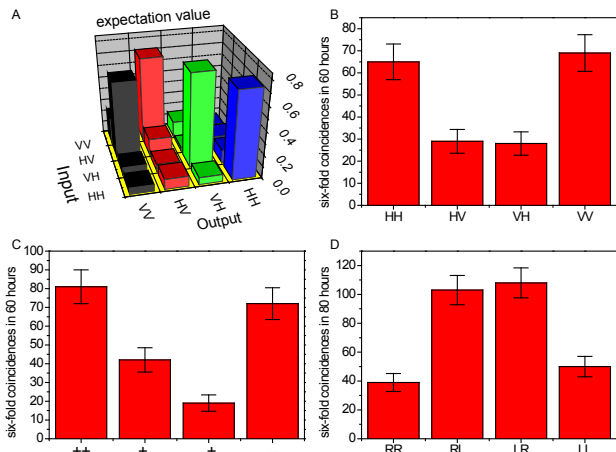


FIG. 3: Experimental results for teleportation-based C-NOT gate. (A) Experimental results for truth table of the C-NOT gate. The first qubit is the target and the second is the control qubit. In the data, we considered the corresponding unitary transformation depending on the type of coincidence at the BSM ($|+\rangle|+\rangle$, $|+\rangle|-\rangle$, $|-\rangle|+\rangle$, $|-\rangle|-\rangle$). The average fidelity for the truth table is 0.72 ± 0.05 . (B) Experimental results for fidelity measurements of entangled output states. Basis $|H\rangle/|V\rangle$ is used for the measurements of $\langle\hat{\sigma}_z\hat{\sigma}_z\rangle$; (C) $|+\rangle/|-\rangle$ for $\langle\hat{\sigma}_x\hat{\sigma}_x\rangle$; (D) $|L\rangle/|R\rangle = \frac{1}{\sqrt{2}}(|H\rangle \pm i|V\rangle)$ for $\langle\hat{\sigma}_y\hat{\sigma}_y\rangle$. The measured expectation values are: (B) 0.403 ± 0.066 (C) 0.462 ± 0.057 and (D) -0.434 ± 0.062 . All errors are statistical and correspond to ± 1 standard deviations.

the in-principle demonstration of the protocol will not be affected since the unsuccessful measurements can be thought of as a photon loss error and will not affect the fidelity of final output. Furthermore, when including the nonlinearity of the detection process, it is, in principle, possible to construct complete BSMs with increasing resources [34].

C. Experimental results

The projective BSMs between the data input photon 1 (2) and photon 3 (5) of the cluster state leave the remaining photons of the cluster state 4&6 in the state $|out\rangle_{46}$ up to a unitary transformation. This is the desired final state after performing a C-NOT operation on photons 1&2. To demonstrate that our teleportation-based C-NOT gate protocol works for a general unknown polarization state of photons 1&2, we measure the truth table of our gate. That is, we measure the output for all possible combinations of the two-qubit input in the computational basis. However, this is not sufficient to show the quantum characteristic of a C-NOT gate. The remarkable feature of a C-NOT gate is its ability to entangle two separable qubits. Thus, to fully demonstrate the successful operation of our protocol, we perform the

entangling operation:

$$|H\rangle_T \otimes \frac{1}{\sqrt{2}}(|H\rangle_C + |V\rangle_C) \xrightarrow{C-NOT} \frac{1}{\sqrt{2}}(|H\rangle_T|H\rangle_C + |V\rangle_C|V\rangle_C) = |\Phi^+\rangle_{TC} \quad (4)$$

We quantify the quality of our output state by looking at the fidelity as defined by $F = \text{Tr}(\hat{\rho}|out\rangle\langle out|)$ where $|out\rangle$ is the theoretically desired final state and $\hat{\rho}$ is the density matrix of the experimental output state.

Here, we discuss the fidelity measurements for the truth table. Conditional on detecting a fourfold coincidence of the two BSMs, we analyze the output photons 4&6 in the computational H/V basis. The measurement results are shown in Fig. 3A, where the corresponding unitary transformation according to different results of the BSMs have been considered. The experimental integration time for each possible combination of the input photons was about 50 hours, and we recorded about 120 desired two-qubit events. In the experiment, we obtained an average fidelity of $F_{z4'z6'} = 0.72 \pm 0.05$ for the output states of the truth table, which is defined as

$$F_{z4'z6'} = 1/4[P(HH|HH) + P(VH|VH) + P(VV|HV) + P(HV|VV)]. \quad (5)$$

Here P represents the probability of obtaining the corresponding output state under the specified input state. For example, $P(VV|HV)$ represents the probability of the case that the output state is $|V\rangle_{4'}|V\rangle_{6'}$ when the input state is $|H\rangle_1|V\rangle_2$.

Next, we demonstrate the entangling capability of the gate. This can be seen by a closer look at the fidelity:

$$F = \text{Tr}(\hat{\rho}|\Phi^+\rangle\langle\Phi^+|) = \frac{1}{4}\text{Tr}\left(\hat{\rho}(\hat{I} + \hat{\sigma}_x\hat{\sigma}_x - \hat{\sigma}_y\hat{\sigma}_y + \hat{\sigma}_z\hat{\sigma}_z)\right). \quad (6)$$

This implies that by measuring the expectation values $\langle\hat{\sigma}_x\hat{\sigma}_x\rangle$, $\langle\hat{\sigma}_y\hat{\sigma}_y\rangle$, $\langle\hat{\sigma}_z\hat{\sigma}_z\rangle$, we can directly obtain the fidelity of the entangled output state. The experimental results for the correlated local measurement settings are illustrated in Fig. 3. The integration time for the first two settings was about 60 hours and for the third setting about 80 hours. Using Eq. 6, we find a fidelity of 0.575 ± 0.027 , which is above 0.50 and thus proves genuine two-photon entanglement in the output states [35].

All experimental results are calculated directly from the original data and no noise contributions have been subtracted. The imperfect fidelity is due to several reasons. First, the imperfect preparation of the cluster state is the main limitation for the non-ideal C-NOT gate. Second, the large pump power double-pair-emission contributes significantly to the noise, which can be seen from the reduction of teleportation fidelity with or without the third pair. Furthermore, the interference visibility is limited since the complex phase compensations drift over the long measurement times. Imperfect input states also

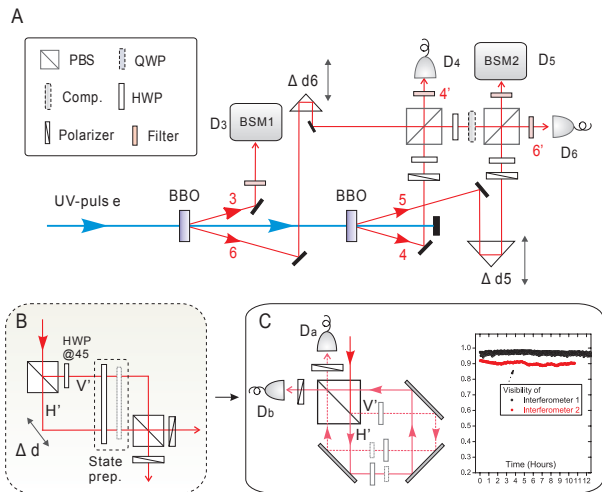


FIG. 4: Schematic of the experimental setup. (A) Femtosecond UV pulses pass through two BBO crystals to create two pairs of entangled photons. Two polarizers are inserted in the arms of 3 and 4 to prepare single photons in $|+\rangle = (1/\sqrt{2})(|H\rangle + |V\rangle)$. (B) Photons 3 and 5 are sent through Mach-Zehnder-type interferometers to perform the spatial-polarization bell-state measurement (BSM). Polarization and spatial qubit transformation happens at the first PBS, and BSM happens at the second PBS. (C) In the experiment, we use an ultra-stable Sagnac configuration interferometer to satisfy the desired high stability.

reduce the quality of our output states. Note that we achieve a better fidelity for the truth table than for the entangling case. This is because in the latter case, the fidelity depends on the interference visibility at the PBS of the BSM. All given errors are of statistical nature and correspond to ± 1 standard deviations.

III. DEMONSTRATION OF THE C-PHASE GATE WITH HYPERENTANGLEMENT

With the help of hyper-entanglement, we are able to tackle the problem of low counting rates in the six-photon experiment [36]. More importantly, it is proved that the GC scheme with hyperentanglement can be extended to implement universal quantum computation based on the so-called “linked-state” [13]. The “linked-state” consists of chains of photons. Every single logical qubit corresponds to a chain, where the spatial degree of freedom of each photon is maximally entangled with the polarization of the next photon. The chains are linked according to the circuit which one wishes to process. Once this state has been successfully prepared, the computation can be realized deterministically by a sequence of teleportation steps and complete single-photon spatial-polarization BSMs [13, 37].

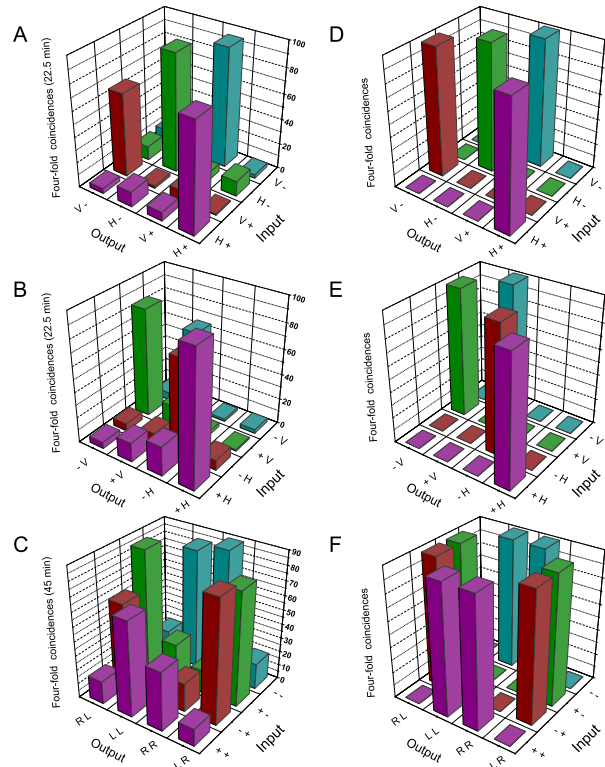


FIG. 5: Experimental evaluation of the quality of the C-phase gate. Data for $F_{z4'x6'}$ and $F_{x4'z6'}$ are measured for 22.5 minutes respectively, and data for $F_{x4'x6'}$ are measured for 45 minutes. (A) Experimental values for measurements of $F_{z4'x6'}$. (B) Experimental values for measurements of $F_{x4'z6'}$. (C) Experimental values for measurements of $F_{x4'x6'}$. (D) Theoretical values for $F_{z4'x6'}$. (E) Theoretical values for $F_{x4'z6'}$. (F) Theoretical values for $F_{x4'x6'}$.

A. The creation of the hyper-entangled four-qubit state $|\chi'\rangle$

In the experiment, we use $|\chi'\rangle$ (Eq. (3)) to teleport the input qubits through a C-Phase gate. In $|\chi'\rangle$, qubits 3, 5 are encoded on the spatial modes of photons and qubits 4', 6' are encoded on the polarization degree of freedom of photons (See Fig. 1A). A schematic of the experimental setup is shown in Fig. 4. A pulsed ultraviolet laser beam passes through two BBO crystals to create two pairs of entangled photons. The first pair is prepared in the state $|\Phi^+\rangle_{36}$. The second pair is disentangled with polarizers and initialized in the state $|+\rangle_4|+\rangle_5$. Then photons 4, 6 and 5, 6 are overlapped on two polarizing beam splitters (PBS) to prepare a four-photon entangled state [40]:

$$|\lambda\rangle = \frac{1}{2} [|H\rangle_3 |H\rangle_{4'} (|H\rangle_5 |H\rangle_{6'} + |V\rangle_5 |V\rangle_{6'}) + |V\rangle_3 |V\rangle_{4'} (|H\rangle_5 |H\rangle_{6'} - |V\rangle_5 |V\rangle_{6'})]. \quad (7)$$

We find the fidelity $F = \text{Tr}(|\lambda\rangle\langle\lambda| \rho_{exp})$ of the prepared state to be 0.71 ± 0.01 , which is above 0.5 by 21 standard

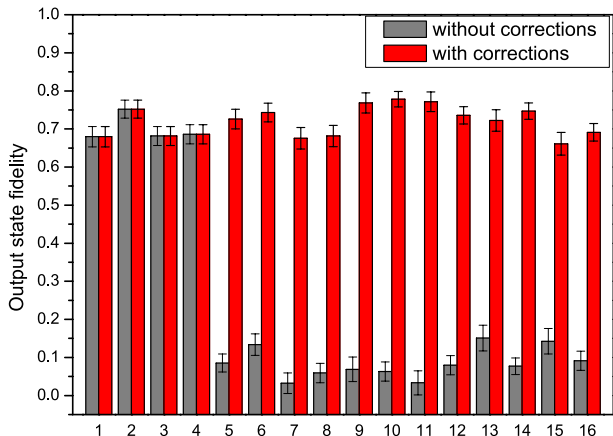


FIG. 6: The fidelity with the expected state before and after the correction operations. The input control and target qubit are both in the state $|+\rangle$, so the output state is expected to be $\frac{1}{\sqrt{2}}(|H+\rangle + |V-\rangle)$. The fidelity is much higher after correction operations. The 16 cases correspond to the 16 different outputs of the two BSMs (see TABLE I in *Appendix*)

deviations and thus proves the genuine four-qubit entanglement in the state [41]. Based on the state $|\lambda\rangle$, we place a PBS in each output of photons 3 & 5. Since the PBS transmits H and reflects V polarization, the H -polarized photon will go to one path and V -polarized photon will go to the other path. If we denote the levels of spatial qubits as $|H'\rangle$ for the first path and $|V'\rangle$ for the second path, $|\lambda\rangle$ will be converted to:

$$|\tilde{\chi}\rangle = \frac{1}{2}[|H'\rangle_3 |H\rangle_{4'} (|H'\rangle_5 |H\rangle_{6'} + |V'\rangle_5 |V\rangle_{6'}) + |V'\rangle_3 |V\rangle_{4'} (|H'\rangle_5 |H\rangle_{6'} - |V'\rangle_5 |V\rangle_{6'})], \quad (8)$$

which is equivalent to $|\chi'\rangle$, except for that qubits 3 and 5 are defined on the spatial degrees of freedom of photons.

B. Teleporting two qubits through a C-Phase gate

We now discuss the preparation of input qubits and the implementation of BSMs. In the experiment, the polarization mode of photon 3 is used as the input target qubit $|T\rangle_1$ and the polarization mode of photon 5 is used as the input control qubit $|C\rangle_2$. As shown in Fig. 4B, by placing HWPs oriented at 45° with respect to the horizontal direction in the spatial mode $|V'\rangle_3$ and $|V'\rangle_5$, the $|V\rangle$ component of photons 3 and 5 will be converted to $|H\rangle$. In this way, the qubits $|T\rangle_1$ and $|C\rangle_2$ to be teleported are both prepared in the initial state $|H\rangle$. Then, by using a combination of HWPs and QWPs, we can prepare arbitrary input states $|T\rangle_1$ and $|C\rangle_2$. The required complete spatial-polarization BSMs are realized by two single photon interferometers (see Fig. 4B). Here Bell

states are denoted as

$$|\Phi^\pm\rangle_i = \frac{1}{\sqrt{2}}(|H\rangle_i |H'\rangle_i \pm |V\rangle_i |V'\rangle_i),$$

$$|\Psi^\pm\rangle_i = \frac{1}{\sqrt{2}}(|H\rangle_i |V'\rangle_i \pm |V\rangle_i |H'\rangle_i), \quad (9)$$

where $i = 3, 5$. By matching the two spatial modes in the Bell states at a PBS, $|\Phi^\pm\rangle_i$ will appear as $|\pm\rangle_i$ in one output port of the PBS, while $|\Psi^\pm\rangle_i$ will appear as $|\pm\rangle_i$ in the other output port. Experimentally, we discriminate these situations to implement a complete BSM and make the corresponding corrections according to different measurement results (see TABLE I in *Appendix*).

Since single photon interferometers are required to implement BSMs, in the experiment we utilize an ultra-stable Sagnac configuration interferometer [42–44] to satisfy the desired high stability. As depicted in Fig. 4C, the H component of the input qubit is transmitted and propagates through the interferometer in the counterclockwise direction, while the V component is reflected and propagates through the interferometer in the clockwise direction. If the setup is adjusted well, the interference will occur when the two spatial modes match at the same PBS. Experimentally, the interferometers can be ultra-stable for about ten hours [44].

C. Experimental results

To evaluate the performance of the C-phase gate, we obtain the upper and lower bounds of the quantum process fidelity and entangling capability with a recent method [45]. Let us define the fidelities as

$$F_{z4'x6'} = 1/4[P(H + |H+\rangle) + P(H - |H-\rangle) + P(V - |V+\rangle) + P(V + |V-\rangle)],$$

$$F_{x4'z6'} = 1/4[P(+H| + H) + P(-V| + V) + P(-H| - H) + P(+V| - V)], \quad (10)$$

where each P has the same definition as in Eq. (5). When the results of Bell state measurements are $|\Phi^+\rangle_3$ and $|\Phi^+\rangle_5$, the experimental results to calculate $F_{z4'x6'}$ and $F_{x4'z6'}$ are depicted in Fig. 5A and 5B. In our experiment, $F_{z4'x6'}$ and $F_{x4'z6'}$ result in 0.79 ± 0.02 and 0.82 ± 0.02 , respectively. The upper and lower bounds of the gate fidelity can be obtained from these two fidelities as follows [45]:

$$(F_{z4'x6'} + F_{x4'z6'} - 1) \leq F_{process} \leq \min(F_{z4'x6'}, F_{x4'z6'}). \quad (11)$$

By substituting the experimental results into the above inequality, we obtain the result that the gate fidelity lies between 0.61 ± 0.03 and 0.79 ± 0.02 . Since the fidelity of entanglement generation is at least equal to the process fidelity, the lower bound above also defines the lower bound of the gate's *entanglement capability*. In terms of the concurrence C that the gate can generate from product state inputs, the minimal entanglement capability is

depicted by [45]:

$$C \geq 2F_{process} - 1 \geq 2(F_{z4'x6'} + F_{x4'z6'}) - 3. \quad (12)$$

We obtain the result that the lower bound of the concurrence is 0.22 ± 0.06 , which is larger than zero and thus sufficient to confirm the entanglement capability of our gate. The imperfection of our gate is mainly due to undesired H/V components caused by high-order photon emissions and partial distinguishability of independent photons interfered on the PBSs.

Furthermore, we demonstrate that quantum parallelism has been achieved in our C-phase gate, thus proving that the gate can not be reproduced by local operations and classical communications [25]. As discussed in ref. [25], quantum parallelism is achieved if the average fidelity of the three distinct conditional local operations exceeds $2/3$, where $F_{z4'x6'}$, $F_{x4'z6'}$ are two of these required fidelities and the third required fidelity is

$$F_{x4'x6'} = \frac{1}{4}[P(RR/++) + P(LL/++) + P(RL/+-) + P(LR/+-) + P(RL/-+) + P(LR/--) + P(RR/--) + P(LL/--)]. \quad (13)$$

In our experiment, $F_{x4'x6'}$ is 0.81 ± 0.02 calculated from the data depicted in Fig. 5C. The average value of $F_{z4'x6'}$, $F_{x4'z6'}$ and $F_{x4'x6'}$ is 0.80 ± 0.01 , clearly exceeding the boundary of $2/3$ and thus proving quantum parallelism in our gate.

In order to verify the deterministic character of the C-Phase gate, we have implemented corrections passively according to different results of BSMS. Both the qubits $|T\rangle_1$ and $|C\rangle_2$ are prepared as the state $|+\rangle$. After a C-Phase gate, theoretically the state of these two qubits should be $\frac{1}{\sqrt{2}}(|H+\rangle + |V-\rangle)$. As depicted in Fig. 6, without corrections the average fidelity of the output state is only 0.24 ± 0.01 . However, with corrections according to the different results of BSMS, we achieve a state with a fidelity of 0.72 ± 0.01 . This agrees with the theoretical expectation. In the future, with the techniques of active feed-forward developed in [46], one can expect to achieve a teleportation-based deterministic C-Phase gate.

IV. DISCUSSION

In summary, with two different approaches, we have demonstrated in principle the feasibility of the GC scheme. By using the six-photon architecture, we have experimentally realized a C-NOT gate based on quantum teleportation. The truth table of the gate has

been measured and the ability to entangle two separable qubits has been demonstrated. With a hyper-entangled four-photon cluster state and ultra-stable single-photon spatial-polarization BSM, we have realized and characterized a teleportation-based quantum optical C-Phase gate.

Below we list some open questions which need to be studied in order to make an advanced optical system in the future. The off-line resource states used in the current experiment are equivalent to four-qubit cluster states. It is proved that efficient preparation of cluster states is possible with a detector efficiency above $1/2$ and an arbitrary small source efficiency [47, 48], where an EPR source that emits a vacuum state or a perfect EPR state is required. This type of state should be studied in the future systems of quantum dots and ions. Moreover, efforts should also be focused on the implementation of chip-scale waveguide quantum circuits [49, 50], which can lead to integrated devices. Third, the spatial modes in the hyper-entangled resource states can only be connected to the polarization qubit of the same photon with the current setup. It should be interesting to investigate how to entangle the spatial mode qubit with the polarization qubit of another photon [13]. Fourth, the GC scheme plays an important role not only in the traditional unitary-evolution-based quantum computation, but also measurement-based quantum computation. The demonstration of the GC scheme can be extended to realize universal “linked-state” measurement-based quantum computation by using more qubits. Lastly, due to the preparation of the resource states in an off-line manner and the transversal operating of the gates in GC scheme, one of the distinct advantages of the GC scheme is that it is inherently fault-tolerant. Encoding the logic qubits onto an error-correction code and implementing a fault-tolerant gate following the GC scheme will be an important step towards fault-tolerant quantum computation.

Acknowledgments

We acknowledge Tracy Li for proofreading the manuscript. This work was supported by the National Natural Science Foundation of China, the Chinese Academy of Sciences and the National Fundamental Research Program (under Grant No 2006CB921900), the Fundamental Research Funds for the Central Universities, the European Commission through the ERC Grant and the STREP project HIP. C.W. was additionally supported by the Schlieben-Lange Program of the ESF.

[1] Knill E, Laflamme R, Milburn GJ (2001) A scheme for efficient quantum computation with linear optics. *Nature* **409** 46-52.

[2] Gottesman D, Chuang IL (1999) Demonstrating the viability of universal quantum computation using teleportation and single-qubit operations. *Nature* **402** 390-393.

- [3] Bennett CH, et al. (1993) Teleporting an unknown quantum state via dual classical and Einstein-Podolsky-Rosen channels. *Phys Rev Lett* **70** 1895-1899.
- [4] Bouwmeester D. et al. (1997) Experimental quantum teleportation. *Nature* **390** 575-579.
- [5] O'Brien JL et al. (2003) Demonstration of an all-optical quantum controlled-NOT gate. *Nature* **426** 264-267.
- [6] Gasparoni S et al. (2004) Realization of a photonic controlled-NOT gate sufficient for quantum computation. *Phys. Rev. Lett.* **93** 020504 (2004).
- [7] Fiorentino M, Wong FNC (2004) Deterministic controlled-NOT gate for single-photon two-qubit quantum logic. *Phys. Rev. Lett.* **93** 070502 (2004).
- [8] Langford NK, et al. (2005) Demonstration of a simple entangling optical gate and its use in Bell-state analysis. *Phys Rev Lett* **95** 210504.
- [9] Kiesel N, et al. (2005) Linear optics controlled-phase gate made simple. *Phys Rev Lett* **95** 210505.
- [10] Okamoto R, Hofmann HF, Takeuchi S, Sasaki K (2005) Demonstration of an optical quantum controlled-not gate without path interference. *Phys Rev Lett* **95** 210506.
- [11] Vallone G, Pomarico E, De Martini F, Mataloni P (2008) Active one-way quantum computation with two-photon four-qubit cluster states. *Phys Rev Lett* **100** 160502.
- [12] Lanyon BP, et al. (2009) Simplifying quantum logic using higher-dimensional Hilbert spaces. *Nature Physics* **5** 134-140.
- [13] Yoran N, Reznik B (2003) Deterministic linear optics quantum computation with single photon qubits. *Phys Rev Lett* **91** 037903.
- [14] Nielsen MA (2004) Optical quantum computation using cluster states. *Phys Rev Lett* **93** 040503.
- [15] Browne DE, Rudolph T (2005) Resource-efficient linear optical quantum computation. *Phys. Rev. Lett.* **95** 010501.
- [16] Gilchrist A, Hayes AJF, Ralph TC (2005) Loss-tolerant optical qubits. *Phys. Rev. Lett.* **95** 100501.
- [17] Briegel HJ, Dür W, Cirac JI, and Zoller P (1998) Quantum repeaters: the role of imperfect local operations in quantum communication. *Phys Rev Lett* **81** 5932.
- [18] Gisin N, Ribordy G, Tittel W, Zbinden H (2002) Quantum cryptography. *Rev Mod Phys* **74** 145-195.
- [19] Nielsen MA (2003) Quantum computation by measurement and quantum memory. *Phys Lett A* **308** 96.
- [20] Raussendorf R, Briegel HJ (2001) A one-way quantum computer. *Phys Rev Lett* **86** 5188.
- [21] Childs AM, Leung DW, Nielsen MA (2005) Unified derivations of measurement-based schemes for quantum computation. *Phys Rev A* **71** 032318.
- [22] Verstraete F, Cirac JI (2004) Valence-bond states for quantum computation. *Phys Rev A* **70** 060302(R).
- [23] Barenco A, et al. (1995) Elementary gates for quantum computation. *Phys Rev A* **52** 3457-3467.
- [24] Kwiat PG (1997) Hyper-entangled states. *J. Mod. Opt.* **44** 2173-2184.
- [25] Hofmann HF (2005) Quantum parallelism of the controlled-NOT operation: An experimental criterion for the evaluation of device performance. *Phys Rev A* **72** 022329.
- [26] Briegel HJ, Raussendorf R (2001) Persistent entanglement in arrays of interacting particles. *Phys Rev Lett* **86** 910-913.
- [27] Kwiat PG, et al. (1995) New high-intensity source of polarization-entangled photon pairs. *Phys Rev Lett* **75** 4337-4341.
- [28] Zhang Q, et al. (2006) Experimental quantum teleportation of a two-qubit composite system. *Nature Physics* **2** 678-682.
- [29] Lu C-Y, et al. (2007) Experimental entanglement of six photons in graph states. *Nature Physics* **3** 91-95.
- [30] Hofmann HF, Takeuchi S (2002) Quantum phase gate for photonic qubits using only beam splitters and postselection. *Phys. Rev. A* **66** 024308.
- [31] Kiesel N, et al. (2005) Experimental analysis of a four-qubit photon cluster state. *Phys Rev Lett* **95** 210502.
- [32] Goebel AM, et al. (2008) Multistage entanglement swapping. *Phys Rev Lett* **101** 080403.
- [33] Pan J-W, Zeilinger A (1998) Greenberger-Horne-Zeilinger-state analyzer. *Phys Rev A* **57** 2208-2211.
- [34] Kok P, et al. (2007) Linear optical quantum computing with photonic qubits. *Rev Mod Phys* **79** 135-174.
- [35] Gühne O, et al. (2002) Detection of entanglement with few local measurements. *Phys Rev A* **66** 062305.
- [36] Tokunaga Y, Yamamoto T, Koashi M, Imoto N (2005) Simple experimental scheme of preparing a four-photon entangled state for the teleportation-based realization of a linear optical controlled-NOT gate. *Phys Rev A* **71** 030301(R).
- [37] Mor T, Yoran N (2006) Methods for scalable optical quantum computation. *Phys Rev Lett* **97** 090501.
- [38] Boschi D, Branca S, Martini F De, Hardy L, Popescu S (1998) Experimental realization of teleporting an unknown pure quantum state via dual classical and Einstein-Podolsky-Rosen channels. *Phys Rev Lett* **80** 1121.
- [39] Zukowski M, Zeilinger A, Weinfurter H (1995) Entangling photons radiated by independent pulsed sources. *Ann NY Acad Sci* **755** 91-102.
- [40] Tokunaga Y, Kuwashiro S, Yamamoto T, Koashi M, Imoto N (2008) Generation of high-fidelity four-photon cluster state and quantum-domain demonstration of one-way quantum computing. *Phys Rev Lett* **100** 210501.
- [41] Tóth G, Gühne O (2005) Detecting genuine multipartite entanglement with two local measurements. *Phys Rev Lett* **94** 060501.
- [42] Nagata T, Okamoto R, O'Brien JL, Sasaki K, Takeuchi S (2007) Beating the standard quantum limit with four-entangled photons. *Science* **316** 726-729.
- [43] Almeida MP, et al. (2007) Environment-induced sudden death of entanglement. *Science* **316** 579-582.
- [44] Gao W-B, et al. (2010) Experimental demonstration of a hyper-entangled ten-qubit Schrödinger cat state. *Nature Physics* **6** 331-335.
- [45] Hofmann HF (2005) Complementary classical fidelities as an efficient criterion for the evaluation of experimentally realized quantum operations. *Phys Rev Lett* **94** 160504.
- [46] Prevedel R, et al. (2007) High-speed linear optics quantum computing using active feed-forward. *Nature* **445** 65-69.
- [47] Varnava M, Browne DE, Rudolph T (2008) How good must single photon sources and detectors be for efficient linear optical quantum computation? *Phys. Rev. Lett.* **100** 060502.
- [48] Wei Z-H, Han Y-J, Oh CH, Duan L-M (2010) Improving noise threshold for optical quantum computing with the EPR photon source, *Phys. Rev. A* **81** 060301.
- [49] Politi A, Cryan MJ, Rarity JG, Yu S. Y., O' Brien JL (2008) Silica-on-silicon Waveguide quantum circuits. *Science* **320** 646.
- [50] Matthews JCF, Politi A, Stefanov A, O' Brien JL (2009)

Manipulating multi-photon entanglement in waveguide quantum circuits. *Nature Photonics* **3** 346.

Appendix

A. Teleportation-based C-NOT gate

Here, we describe in detail the scheme of a teleportation-based C-NOT gate. We give a step by step analyses of its implementation with our setup, shown in Fig. 2 in the main article.

We align each β -barium borate (BBO) crystal carefully to produce a pair of polarization entangled photons i and j in the state:

$$|\Psi^+\rangle_{ij} = \frac{1}{\sqrt{2}} (|H\rangle_i |H\rangle_j + |V\rangle_i |V\rangle_j) \quad (\text{S.1})$$

We use the method described in ref. [1–4] to prepare the cluster state $|\chi\rangle$. Initially, photons 3, 4, 5 and 6 are in the state:

$$\begin{aligned} & |\Psi^+\rangle_{34} \otimes |\Psi^+\rangle_{56} \\ &= \frac{1}{2} (|H\rangle_3 |H\rangle_4 |H\rangle_5 |H\rangle_6 + |H\rangle_3 |H\rangle_4 |V\rangle_5 |V\rangle_6 + \\ & \quad |V\rangle_3 |V\rangle_4 |H\rangle_5 |H\rangle_6 + |V\rangle_3 |V\rangle_4 |V\rangle_5 |V\rangle_6). \end{aligned} \quad (\text{S.2})$$

We direct photons 4 and 6 to the two input modes of a partially polarizing beam splitters (PPBS), respectively. The transmission T_H (T_V) of horizontally (vertically) polarized light at the PPBS is 1 (1/3), and we thus get

$$\begin{aligned} & \rightarrow \frac{1}{2} (|H\rangle_3 |H\rangle_{4'} |H\rangle_5 |H\rangle_{6'} + \frac{1}{\sqrt{3}} |H\rangle_3 |H\rangle_{4'} |V\rangle_5 |V\rangle_{6'} \\ & \quad + \frac{1}{\sqrt{3}} |V\rangle_3 |V\rangle_{4'} |H\rangle_5 |H\rangle_{6'} \\ & \quad - \frac{1}{3} |V\rangle_3 |V\rangle_{4'} |V\rangle_5 |V\rangle_{6'}). \end{aligned} \quad (\text{S.3})$$

Here we have neglected terms with more than one photon in a single output mode of the PPBS, since in the experiment we post select only terms that lead to a six-fold coincidence.

In order to symmetrize the state we place a PPBS' ($T_H = 1/3, T_V = 1$) in each output mode of the PPBS and receive

$$\begin{aligned} & \rightarrow \frac{1}{6} (|H\rangle_3 |H\rangle_{4''} |H\rangle_5 |H\rangle_{6''} + |H\rangle_3 |H\rangle_{4''} |V\rangle_5 |V\rangle_{6''} \\ & \quad + |V\rangle_3 |V\rangle_{4''} |H\rangle_5 |H\rangle_{6''} - |V\rangle_3 |V\rangle_{4''} |V\rangle_5 |V\rangle_{6''}). \end{aligned} \quad (\text{S.4})$$

This is already the desired four-qubit cluster state up to local unitary operations. To bring it to the desired form, we place half-wave plates (HWPs) – with an angle of 22.5° between the fast and the horizontal axis – into arms 3 and 4. This yields

$$\begin{aligned} & \rightarrow (|H\rangle_3 |H\rangle_{4''} + |V\rangle_3 |V\rangle_{4''}) |H\rangle_5 |H\rangle_{6''} \\ & \quad + (|H\rangle_3 |V\rangle_{4''} + |V\rangle_3 |H\rangle_{4''}) |V\rangle_5 |V\rangle_{6''} \\ & = |\chi\rangle_{34''56''}, \end{aligned} \quad (\text{S.5})$$

where we have neglected the overall pre-factor 1/6 and we arrive at the desired ancillary four-photon cluster state $|\chi\rangle$ described in ref. [5].

Photons 1 and 2 constitute the input to our C-NOT gate. We assume that they are in a most general input state $|\Psi_{in}\rangle_{12}$, where:

$$\begin{aligned} |\Psi_{in}\rangle_{ij} &= \alpha |H\rangle_i |H\rangle_j + \beta |H\rangle_i |V\rangle_j \\ & \quad + \gamma |V\rangle_i |H\rangle_j + \delta |V\rangle_i |V\rangle_j \end{aligned} \quad (\text{S.6})$$

The pre-factors α, β, γ and δ are four arbitrary complex numbers satisfying $|\alpha|^2 + |\beta|^2 + |\gamma|^2 + |\delta|^2 = 1$. Before we proceed, let us define the desired output state after a C-NOT operation:

$$\begin{aligned} |\Psi_{out}\rangle_{ij} &= U^{C-NOT} |\Psi_{in}\rangle_{ij} \\ &= \alpha |H\rangle_i |H\rangle_j + \beta |V\rangle_i |V\rangle_j + \\ & \quad \gamma |V\rangle_i |H\rangle_j + \delta |H\rangle_i |V\rangle_j \end{aligned} \quad (\text{S.7})$$

The target qubit i is flipped on the condition that the control qubit j is in the state $|V\rangle$.

We can now express the combined state of all six photons in terms of Bell states for photons 1&3 and 2&5 and in terms of the desired output state $|\Psi_{out}\rangle_{46}$ for photons 4&6 with corresponding Pauli operations:

$$\begin{aligned} & |\Psi_{in}\rangle_{12} \otimes |\chi\rangle_{3456} = \\ & \quad |\Phi^+\rangle_{13} |\Phi^+\rangle_{25} \quad |\Psi_{out}\rangle_{46} + |\Phi^+\rangle_{13} |\Phi^-\rangle_{25} \quad \hat{\sigma}_z^6 |\Psi_{out}\rangle_{46} \\ & \quad + |\Phi^+\rangle_{13} |\Psi^+\rangle_{25} \quad \hat{\sigma}_x^4 \hat{\sigma}_x^6 |\Psi_{out}\rangle_{46} + |\Phi^+\rangle_{13} |\Psi^-\rangle_{25} \quad \hat{\sigma}_x^4 \hat{\sigma}_x^6 \hat{\sigma}_z^6 |\Psi_{out}\rangle_{46} \\ & \quad + |\Phi^-\rangle_{13} |\Phi^+\rangle_{25} \quad \hat{\sigma}_z^4 \hat{\sigma}_z^6 |\Psi_{out}\rangle_{46} + |\Phi^-\rangle_{13} |\Phi^-\rangle_{25} \quad \hat{\sigma}_z^4 |\Psi_{out}\rangle_{46} \\ & \quad + |\Phi^-\rangle_{13} |\Psi^+\rangle_{25} \quad \hat{\sigma}_x^4 \hat{\sigma}_z^4 \hat{\sigma}_x^6 \hat{\sigma}_z^6 |\Psi_{out}\rangle_{46} + |\Phi^-\rangle_{13} |\Psi^-\rangle_{25} \quad \hat{\sigma}_x^4 \hat{\sigma}_z^4 \hat{\sigma}_x^6 |\Psi_{out}\rangle_{46} \\ & \quad + |\Psi^+\rangle_{13} |\Phi^+\rangle_{25} \quad \hat{\sigma}_x^4 |\Psi_{out}\rangle_{46} + |\Psi^+\rangle_{13} |\Phi^-\rangle_{25} \quad \hat{\sigma}_x^4 \hat{\sigma}_z^6 |\Psi_{out}\rangle_{46} \\ & \quad + |\Psi^+\rangle_{13} |\Psi^+\rangle_{25} \quad \hat{\sigma}_x^6 |\Psi_{out}\rangle_{46} + |\Psi^+\rangle_{13} |\Psi^-\rangle_{25} \quad \hat{\sigma}_x^4 \hat{\sigma}_z^6 |\Psi_{out}\rangle_{46} \\ & \quad + |\Psi^-\rangle_{13} |\Phi^+\rangle_{25} \quad \hat{\sigma}_x^4 \hat{\sigma}_z^4 \hat{\sigma}_z^6 |\Psi_{out}\rangle_{46} + |\Psi^-\rangle_{13} |\Phi^-\rangle_{25} \quad \hat{\sigma}_x^4 \hat{\sigma}_z^4 |\Psi_{out}\rangle_{46} \\ & \quad + |\Psi^-\rangle_{13} |\Psi^+\rangle_{25} \quad \hat{\sigma}_z^4 \hat{\sigma}_x^6 \hat{\sigma}_z^6 |\Psi_{out}\rangle_{46} + |\Psi^-\rangle_{13} |\Psi^-\rangle_{25} \quad \hat{\sigma}_z^4 \hat{\sigma}_x^6 |\Psi_{out}\rangle_{46} \end{aligned} \quad (\text{S.8})$$

With the help of polarizing beam splitters, in our experiment we are able to identify the Bell states $|\Phi^\pm\rangle_{13}$ and $|\Phi^\pm\rangle_{25}$, i.e. we project the combined state of photons 1, 2,

3 and 5 onto one of the four possibilities $|\Phi^\pm\rangle_{13} |\Phi^\pm\rangle_{25}$. We thus have to consider four different results of the BSMs:

Result of BSMS	Output state
$ \Phi^+\rangle_{13} \Phi^+\rangle_{25}$	$ \Psi_{out}\rangle_{46}$
$ \Phi^+\rangle_{13} \Phi^-\rangle_{25}$	$\hat{\sigma}_z^6 \Psi_{out}\rangle_{46}$
$ \Phi^-\rangle_{13} \Phi^+\rangle_{25}$	$\hat{\sigma}_z^4\hat{\sigma}_z^6 \Psi_{out}\rangle_{46}$
$ \Phi^-\rangle_{13} \Phi^-\rangle_{25}$	$\hat{\sigma}_z^4 \Psi_{out}\rangle_{46}$

To receive the desired final state of photons 4 and 6, we have to apply corresponding Pauli operations, depending on the outcome of the BSMS.

B. Teleportation-based C-Phase gate

Similarly to the last section, in the implementation of a teleportation-based C-Phase gate, we also need to apply 16 different Pauli corrections on the output qubits according to 16 possible combinations of outcomes of BSMS. We list the required correction operations in the Table S.1.

measurements	$ \Phi^+\rangle_3$	$ \Phi^-\rangle_3$	$ \Psi^+\rangle_3$	$ \Psi^-\rangle_3$
$ \Phi^+\rangle_5$	I	$Z_{4'}$	$X_{4'}Z_{6'}$	$iY_{4'}Z_{6'}$
$ \Phi^-\rangle_5$	$Z_{6'}$	$Z_{4'}Z_{6'}$	$X_{4'}$	$iY_{4'}$
$ \Psi^+\rangle_5$	$Z_{4'}X_{6'}$	$X_{6'}$	$Y_{4'}Y_{6'}$	$-iX_{4'}Y_{6'}$
$ \Psi^-\rangle_5$	$iZ_{4'}Y_{6'}$	$iY_{6'}$	$-iY_{4'}X_{6'}$	$-X_{4'}X_{6'}$

TABLE S.1: The required correction operations depending on the Bell state measurement results. We define $|\Phi^\pm\rangle_i = \frac{1}{\sqrt{2}}(|H\rangle_i|H'\rangle_i \pm |V\rangle_i|V'\rangle_i)$, $|\Psi^\pm\rangle_i = \frac{1}{\sqrt{2}}(|H\rangle_i|V'\rangle_i \pm |V\rangle_i|H'\rangle_i)$, where $|H'\rangle$ and $|V'\rangle$ are spatial qubits. The 16 cases in Fig. 6 in the main text correspond to the output results: $|\Phi^+\rangle_3|\Phi^+\rangle_5$, $|\Psi^+\rangle_3|\Phi^+\rangle_5$, $|\Phi^+\rangle_3|\Psi^+\rangle_5$, $|\Psi^+\rangle_3|\Psi^+\rangle_5$, $|\Phi^+\rangle_3|\Phi^-\rangle_5$, $|\Psi^+\rangle_3|\Phi^-\rangle_5$, $|\Phi^+\rangle_3|\Psi^-\rangle_5$, $|\Psi^+\rangle_3|\Psi^-\rangle_5$, $|\Phi^-\rangle_3|\Phi^+\rangle_5$, $|\Psi^-\rangle_3|\Phi^+\rangle_5$, $|\Phi^-\rangle_3|\Psi^+\rangle_5$, $|\Psi^-\rangle_3|\Psi^+\rangle_5$, $|\Phi^-\rangle_3|\Phi^-\rangle_5$, $|\Psi^-\rangle_3|\Phi^-\rangle_5$, $|\Phi^-\rangle_3|\Psi^-\rangle_5$, $|\Psi^-\rangle_3|\Psi^-\rangle_5$.

-
- [1] [S1]Langford NK, et al. (2005) Demonstration of a simple entangling optical gate and its use in Bell-state analysis. *Phys Rev Lett* **95** 210504.
 - [2] [S2]Kiesel N, et al. (2005) Linear optics controlled-phase gate made simple. *Phys Rev Lett* **95** 210505.
 - [3] [S3]Okamoto R, Hofmann HF, Takeuchi S, Sasaki K (2005) Demonstration of an optical quantum controlled-not gate without path interference. *Phys Rev Lett* **95** 210506.
 - [4] [S4]Kiesel N, et al. (2005) Experimental analysis of a four-lubit photon cluster state. *Phys Rev Lett* **95** 210502.
 - [5] [S5]Gottesman D, Chuang IL (1999) Demonstrating the viability of universal quantum computation using teleportation and single-qubit operations. *Nature* **402** 390.